Supplementary Materials for

Endothelial caveolin-1 regulates cerebral thrombo-inflammation in acute ischemia/reperfusion injury

Xiaohao Zhang[1,2,3†], Pengyu Gong[4†], Ying Zhao[1†], Ting Wan[1], Kang Yuan[1], Yunyun Xiong[5,6,7], Min Wu[8], Mingming Zha[1], Yunzi Li[1], Teng Jiang[2], Xinfeng Liu[1], Ruidong Ye[1], Yi Xie[1*], Gelin Xu[1*]

[†]Contributed equally.

[*]Corresponding author. E-mail: xy_307@126.com (Y.X.) or gelinxu@nju.edu.cn (G.X.)

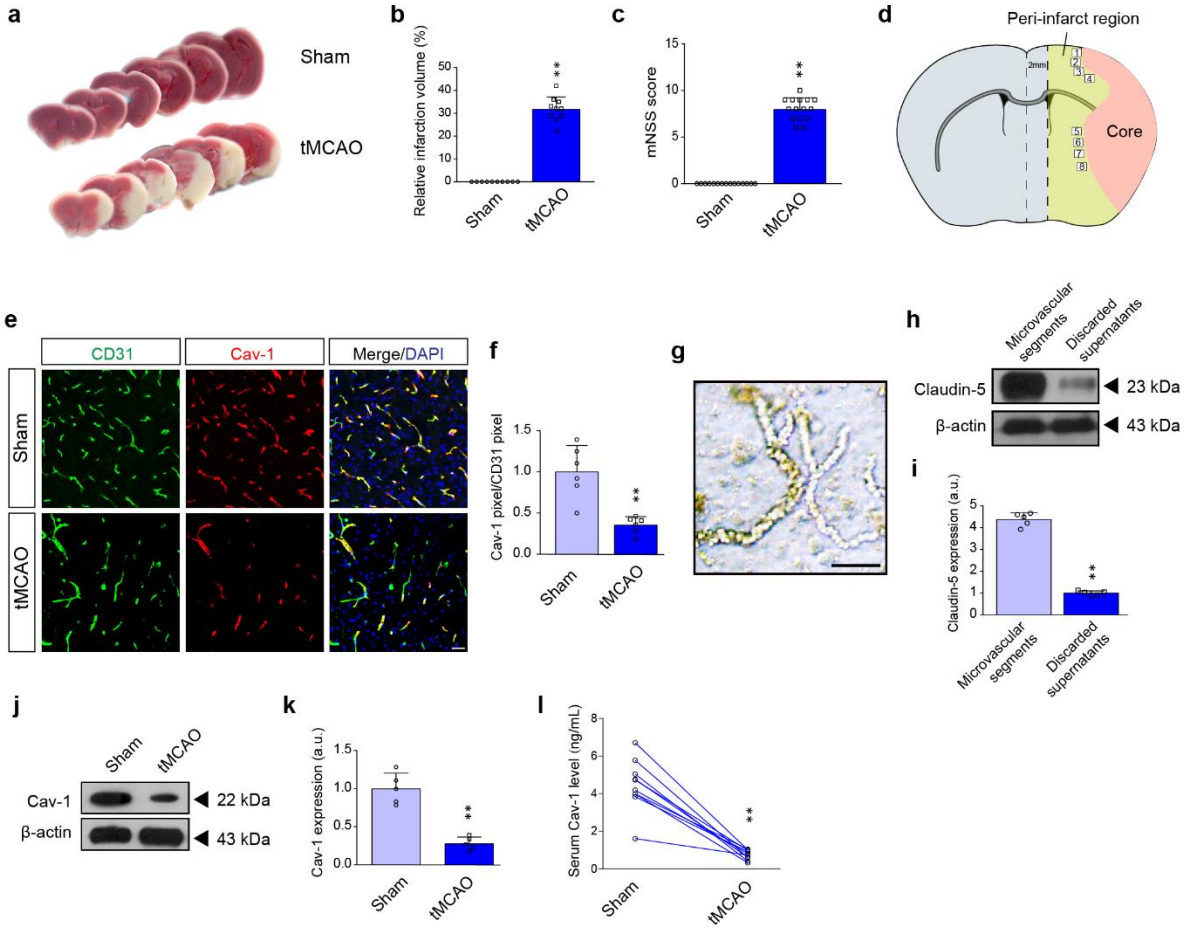

Supplemental Figure 1. Endothelial and serum Cav-1 levels are decreased at tMCAO-24h.

(**a**) Representative images of coronal brain sections stained with TTC [quantified in (**b**); n = 10 in each group; mean ± S.D; ***P* < 0.01 *vs.* sham by unpaired t-test). (**c**) The mNSS score of sham and tMCAO mice 24 h after surgery (n = 15 in each group; mean ± S.D; ***P* < 0.01 *vs.* sham by unpaired t-test). (**d**) Schematic map showing eight fields in the peri-infarct region for immunostaining image acquisition in every sample. (**e, f**) Representative immunostaining images and quantification showing the expression of Cav-1 in endothelial cells ($CD31^+$) (n = 6 in each group; mean ± S.D; ***P* < 0.01 *vs.* sham by unpaired t-test). (**g**) Representative light microscopic image of isolated brain microvessels from the peri-infarct area. (**h, i**) Immunoblotting and quantification showing the expression of endothelial-specific marker Claudin-5 in the isolated microvessels from the peri-infarct tissue 24h after surgery (a pool of 2 mice per sample; n = 5 samples per group; mean ± S.D; ***P* < 0.01 vs. microvascular segments by unpaired t-test). (**j, k**) Immunoblotting and quantification showing the Cav-1 expression in isolated brain microvessels from the peri-infarct tissue (a pool of 2 mice per sample; n = 5 samples per group; ***P* < 0.01 *vs.* sham by unpaired t-test). (**l**) Serum level of Cav-1 in sham and tMCAO mice (n = 8; mean ± S.D; ***P* < 0.01 *vs.* sham by unpaired t-test). Scale bar: 20 μm.

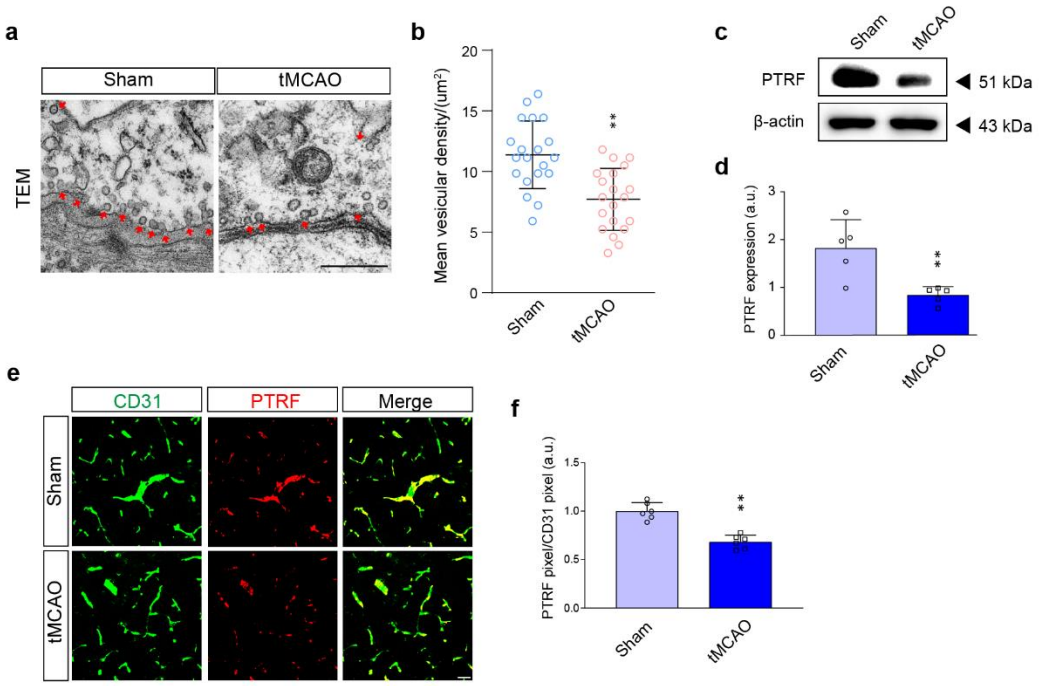

Supplemental Figure 2. Arteriole caveolae are reduced at the peri-infarct region at tMCAO-24h.

(**a**) TEM images showing the alteration of arteriole caveolae (red arrows) [quantified in (**b**); n = 5 mice, 20 arterioles in each group; mean ± S.D; ***P* < 0.01 *vs.* sham by unpaired t-test]. (**c, d**) Immunoblotting and quantification showing the expression of PTRF in isolated brain microvessels from the peri-infarct tissue (a pool of 2 mice per sample; n = 5 samples per group; ***P* < 0.01 *vs.* sham by unpaired t-test). (**e, f**) Representative immunostaining images and qualification showing the expression of PTRF in the endothelium ($CD31^+$) (n = 6 in each group; mean ± S.D; ***P* < 0.01 *vs.* sham by unpaired t-test). Scale bar: 500 nm in (**a**) and 20 μm in (**e**).

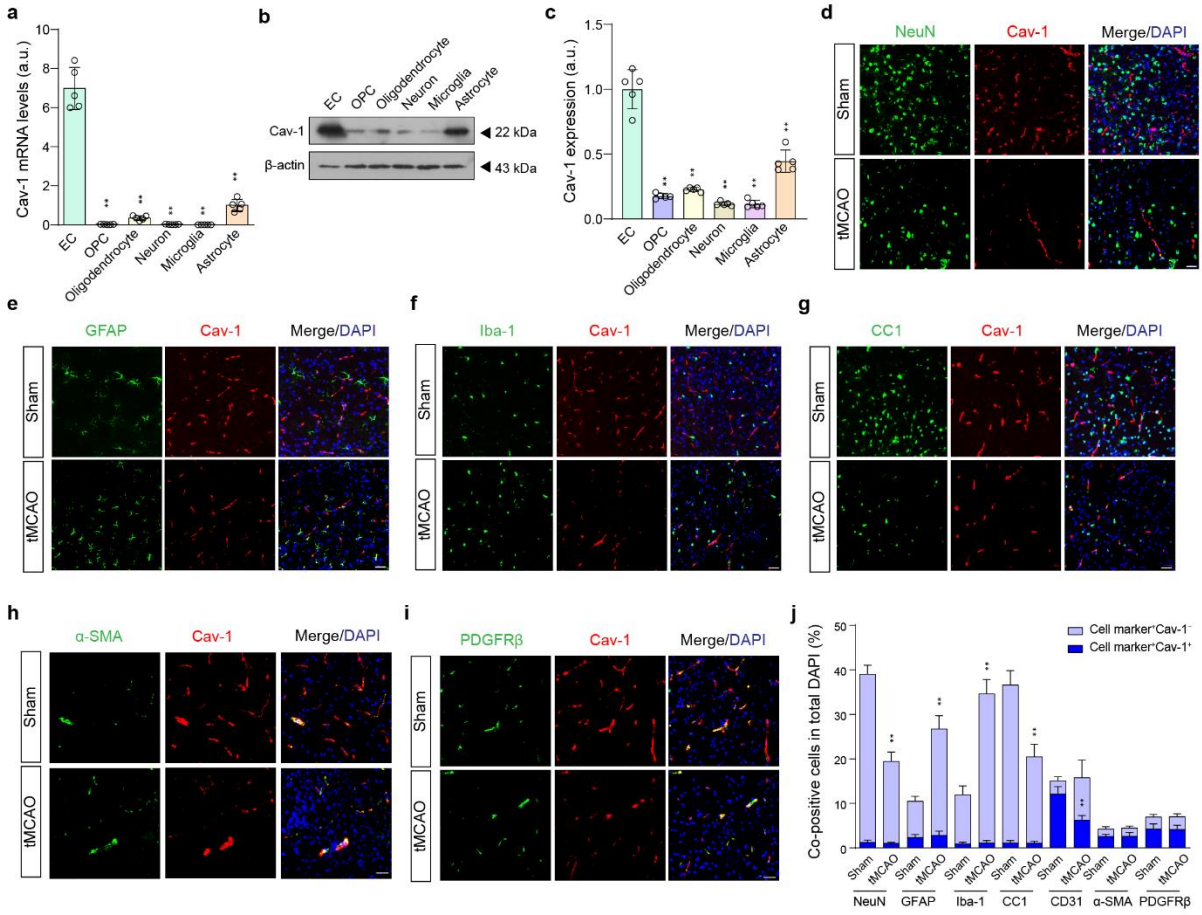

Supplemental Figure 3. The cell-type specificity of Cav-1 expression under physiological and pathological conditions.

(**a–c**) *Cav-1* mRNA and protein levels in primary cultured endothelium, OPC, oligodendrocyte, neuron, microglia, and astrocyte *in vitro* (n = 5 experiments; mean ± S.D; ***P* < 0.01 *vs.* endothelium by one-way ANOVA with Tukey post hoc test). (**d–i**) Double immunostaining of Cav-1 with NeuN (neuron marker), GFAP (astrocyte marker), Iba-1 (microglia marker), CC1 (mature oligodendrocyte marker), α-SMA (vascular smooth muscle cell marker), and PDGFRβ (pericytes marker) at the peri-infarct region 24 h after tMCAO [quantified in (**j**); n = 6 in each group; mean ± S.D; ***P* < 0.01 *vs.* sham by unpaired t-test]. Scale bar, 20 μm.

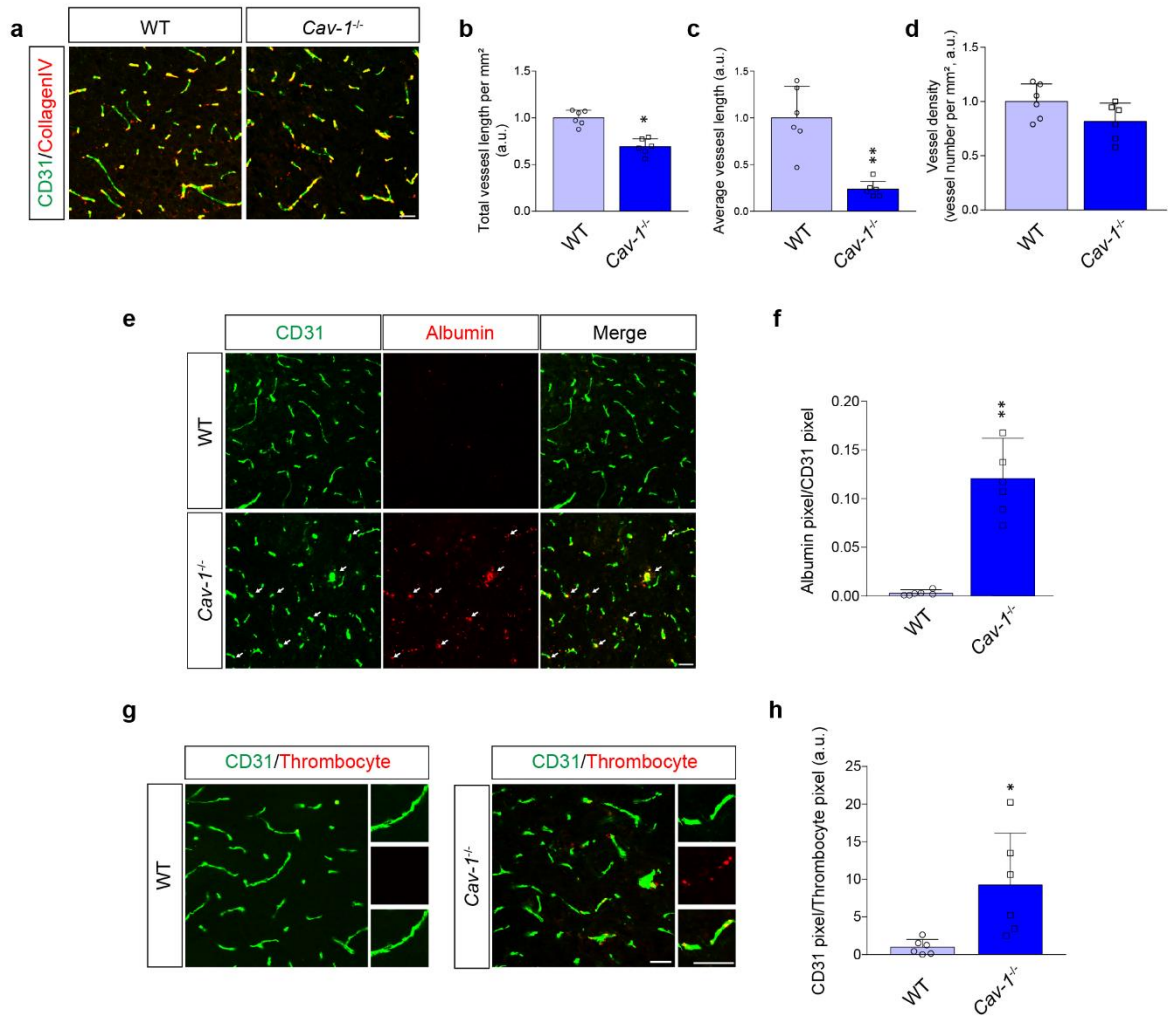

Supplemental Figure 4. Cav-1 deletion induces endothelial pathological changes. (**a**) Representative images of microvessels (CD31$^+$, green; Collagen IV$^+$, red) [quantified in (**b–d**); n = 6 in each group; mean ± S.D; **P* < 0.05, ***P* < 0.01 *vs.* WT mice by unpaired t-test]. (**e, f**) Immunofluorescent images and quantification showing the albumin leakage (red) around CD31$^+$ (green) vessels (n = 6 in each group; mean ± S.D; ***P* < 0.05 *vs.* WT mice by unpaired t-test). (**g, h**) Representative images and quantification showing thrombocytes (red) in the cerebral microvessels (CD31$^+$, green) (n = 6 in each group; mean ± S.D; **P* < 0.05 *vs.* WT mice by unpaired t-test). Scale bar: 20 μm.

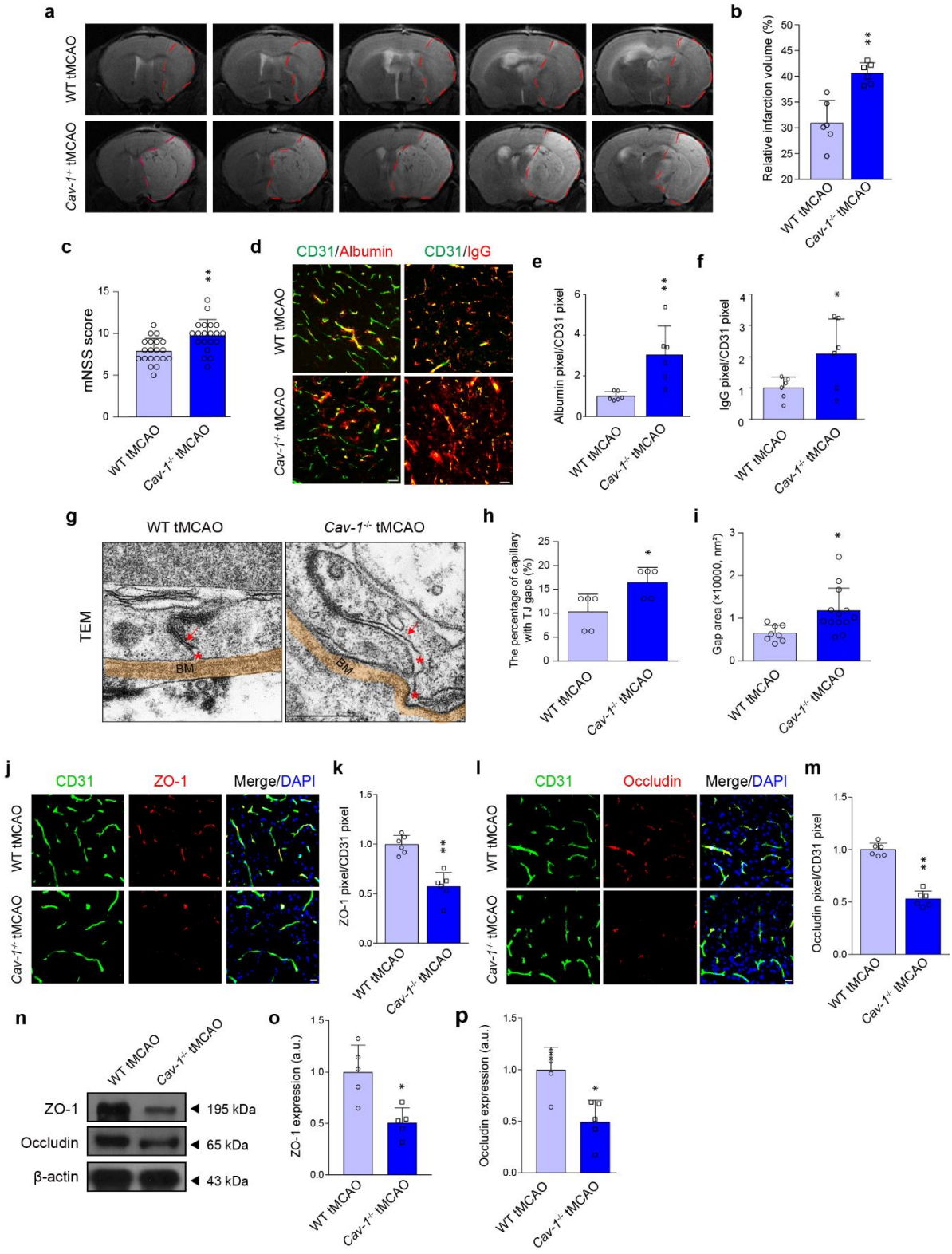

Supplemental Figure 5. Cav-1 deficiency increases the microvascular permeability in tMCAO-24h.

(**a**) Representative images of 5 coronal brain sections in T2 MRI scans of WT tMCAO mice and *Cav-1*$^{-/-}$ tMCAO mice [quantified in (**b**); n = 6 in each group; mean ± S.D; ***P* < 0.01 *vs.* WT tMCAO mice by unpaired t-test]. (**c**) The mNSS score of tMCAO mice of two genotypes 24 h after surgery (n = 20 in each group; mean ± S.D; ***P* < 0.01 *vs.* WT tMCAO mice by unpaired t-test). (**d–f**) Immunofluorescence staining and quantification showing the albumin (red) and IgG leakage (red) around vessels (CD31^{+},

green) at the peri-infarct area 24 h after tMCAO (n = 6 in each group; mean ± S.D; *P < 0.05; **P < 0.01 *vs.* WT tMCAO mice by unpaired t-test). (**g**) TEM images showing endothelial TJ gaps in the peri-infarct area from WT tMCAO and *Cav-1*$^{-/-}$ MCAO mice 24 h after surgery [quantified in (**h, i**); n = 5 mice in each group. Sixteen capillaries were randomly chosen in each mouse; mean ± S.D; *P < 0.05 *vs.* WT tMCAO mice by unpaired t-test]. The red arrows indicate gaps between endothelial cells. The red asterisks indicate gaps between endothelial cells and basal membrane. (**j, i**) Immunofluorescence staining showing the expression of ZO-1 (red) and occludin (red) in the vessels (CD31^{+}, green) at the peri-infarct area [quantified in (**k, m**); n = 6 in each group; mean ± S.D; **P < 0.01 *vs.* WT tMCAO mice by unpaired t-test]. (**n–p**) Immunoblotting and quantitative analysis of TJ protein 24 h after surgery (a pool of 2 mice per sample; n = 5 samples per group; *P < 0.05 *vs.* WT tMCAO mice by unpaired t-test). Scale bar: 500 nm in (**g**) and 20 μm in others. BM, basal membrane.

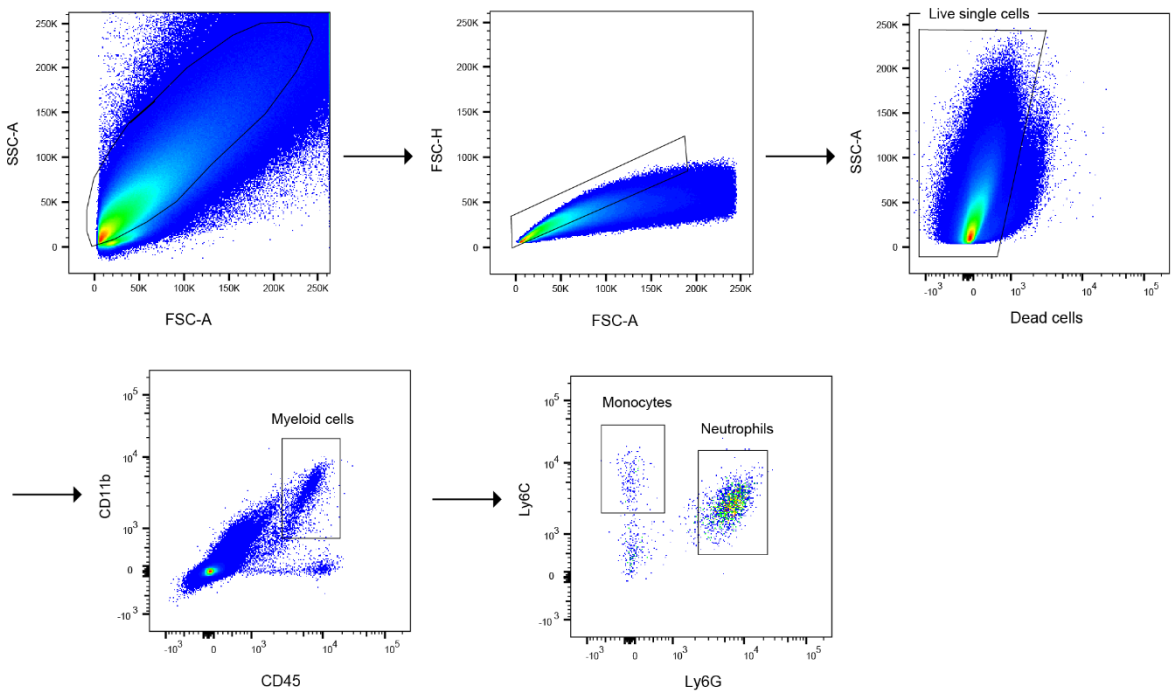

Supplemental Figure 6. Gating strategies for flow cytometry to evaluate myeloid cell infiltration in the ischemic hemisphere at tMCAO-24h.

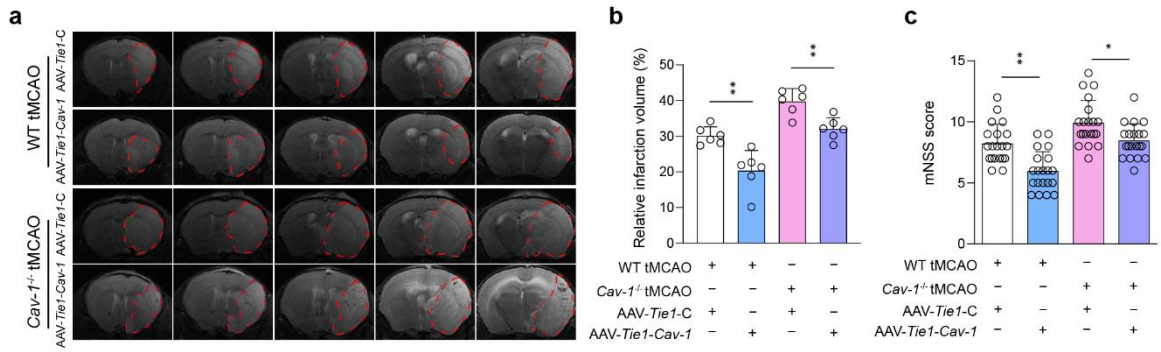

Supplemental Figure 7. AAV-*Tie1-Cav-1* decreases the infarct volume and mNSS score at tMCAO-24h.

(**a**) Representative images of 5 coronal brain sections in T2 MRI scans of wild-type tMCAO and *Cav-1*$^{-/-}$ tMCAO mice transfected with AAV-*Tie1*-C or AAV-*Tie1-Cav-1* [quantified in (**b**); n = 6 in each group; mean ± S.D; ***P* < 0.01 *vs.* AAV-*Tie1*-C-transfected mice by one-way ANOVA with Tukey post hoc test]. (**c**) The mNSS score of wild-type tMCAO and *Cav-1*$^{-/-}$ tMCAO mice transfected with AAV-*Tie1*-C or AAV-*Tie1-Cav-1* (n = 20 in each group; mean ± S.D; **P* < 0.05; ***P* < 0.01 *vs.* AAV-*Tie1*-C-transfected mice by one-way ANOVA with Tukey post hoc test).

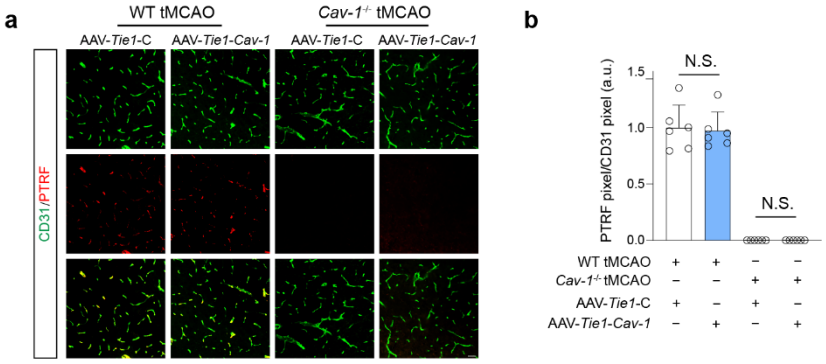

Supplemental Figure 8. AAV-*Tie1-Cav-1* does not affect the PTRF level.

(**a, b**) Representative fluorescent images and qualification of PTRF (red) in microvessels (CD31$^+$, green) at the peri-infarct tissue 24 h after tMCAO (n = 6 in each group; mean ± S.D; one-way ANOVA with Tukey post hoc test). Scale bar: 20 μm.

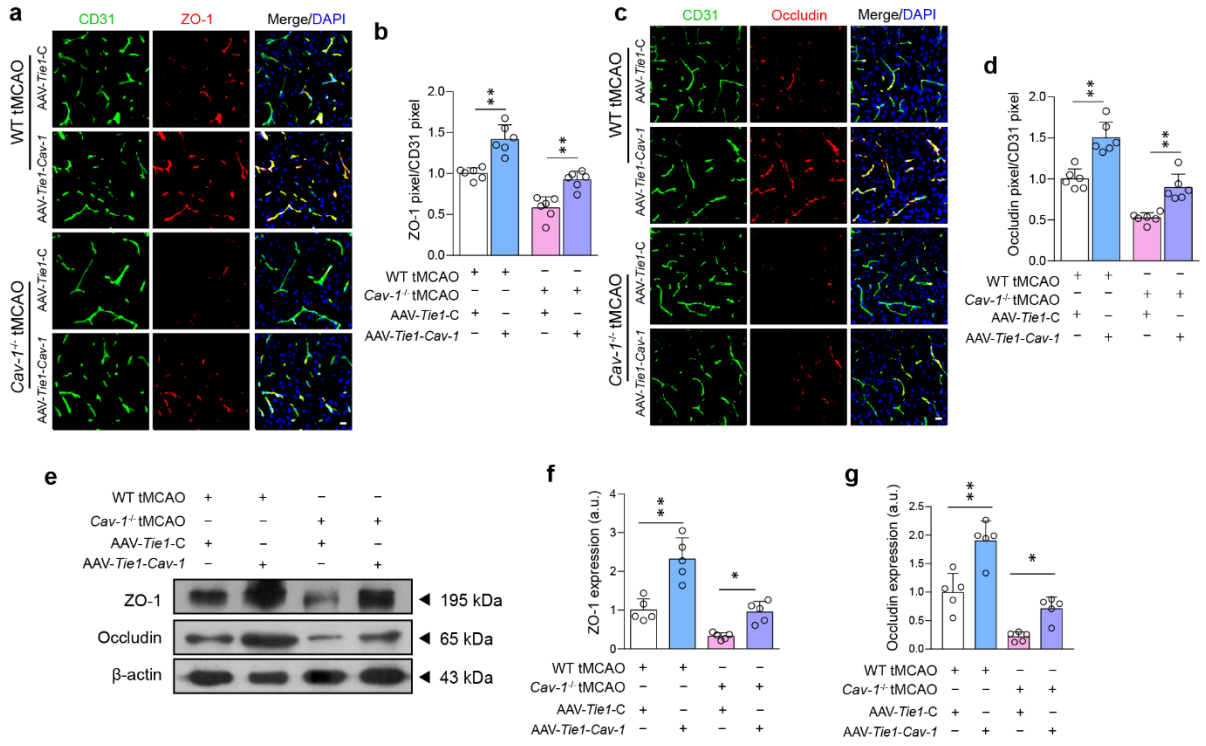

Supplemental Figure 9. AAV-*Tie1-Cav-1* increases TJ protein expression at tMCAO-24h.

(**a, c**) Immunofluorescence staining showing the expression of ZO-1 (red) and occludin (red) in the vessels (CD31$^+$, green) at the peri-infarct area 24 h after tMCAO [quantified in (**b, d**); n = 6 in each group; mean ± S.D; ***P* < 0.01 *vs.* AAV-*Tie1*-C-transfected mice by one-way ANOVA with Tukey post hoc test]. (**e–g**) Quantitative analysis for immunoblotting of TJ proteins 24 h after tMCAO (a pool of 2 mice per sample; n = 5 samples per group; **P* < 0.05; ***P* < 0.01 *vs.* AAV-*Tie1*-C-transfected mice by one-way ANOVA with Tukey post hoc test). Scale bar: 20 μm.

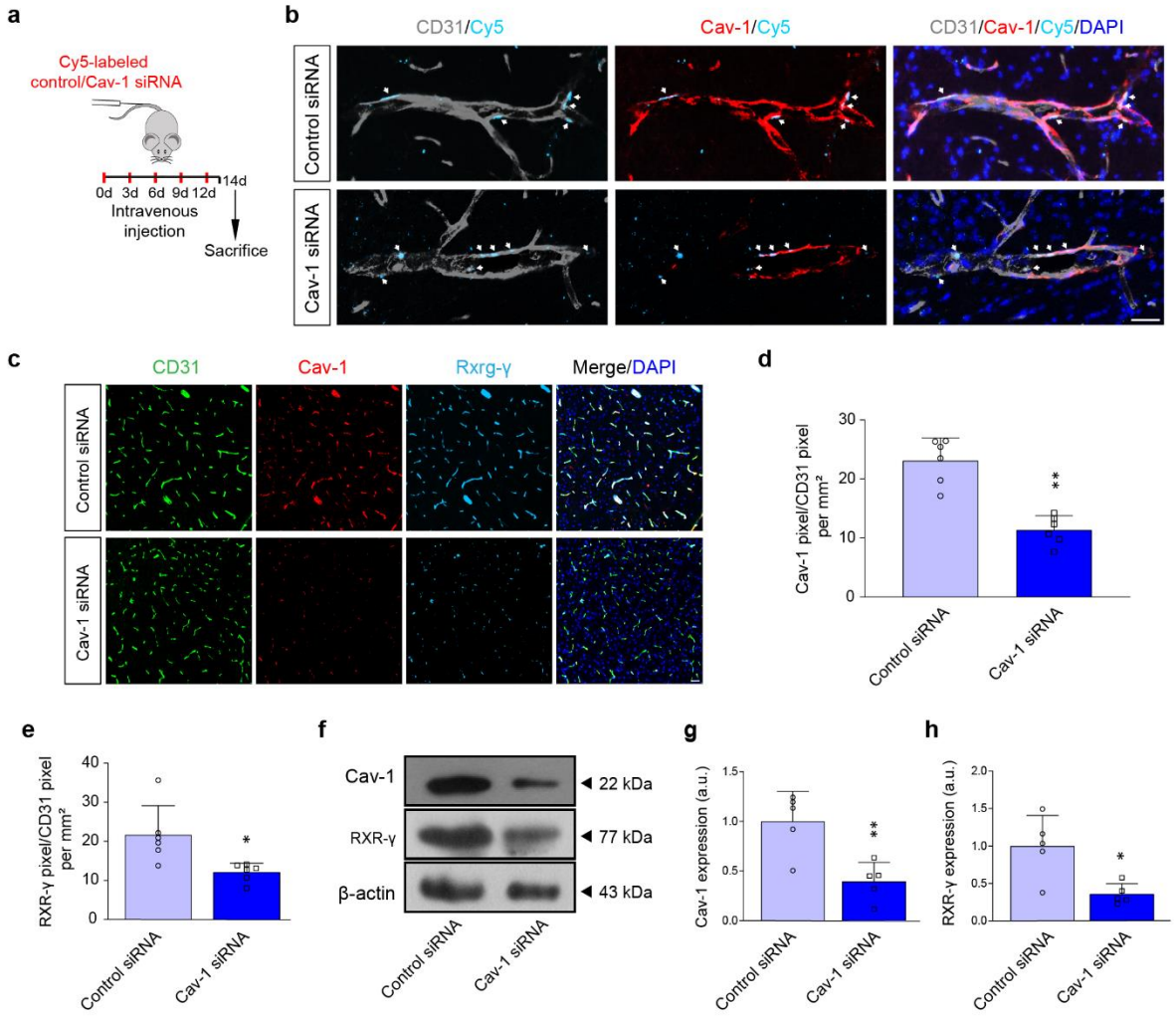

Supplemental Figure 10. Cav-1 siRNA suppresses endothelial Cav-1 as well as RXR-γ expression at tMCAO-24h.

(**a**) Experimental flow chart. (**b**) Representative immunofluorescence staining showing the co-localization of siRNA (cyan), Cav-1 (red) and CD31 (gray) in siRNA-injected WT Sham mice (n = 6 in each group). (**c**) Representative images of immunofluorescence staining for Cav-1 (red) or RXR-γ (cyan) in the cerebral microvessels ($CD31^+$, green) [quantified in (**d, e**); n = 6 in each group; mean ± S.D; **P* < 0.05; ***P* < 0.01 *vs.* control siRNA-injected mice by unpaired t-test]. (**f–h**) Immunoblotting and quantification displaying the expression of Cav-1 and RXR-γ in brain microvascular segments from the 2 groups (a pool of 2 mice per sample; n = 5 samples per group; mean ± S.D; **P* < 0.05; ***P* < 0.01 *vs.* control siRNA-injected mice by unpaired t-test). Scale bar: 20 μm.

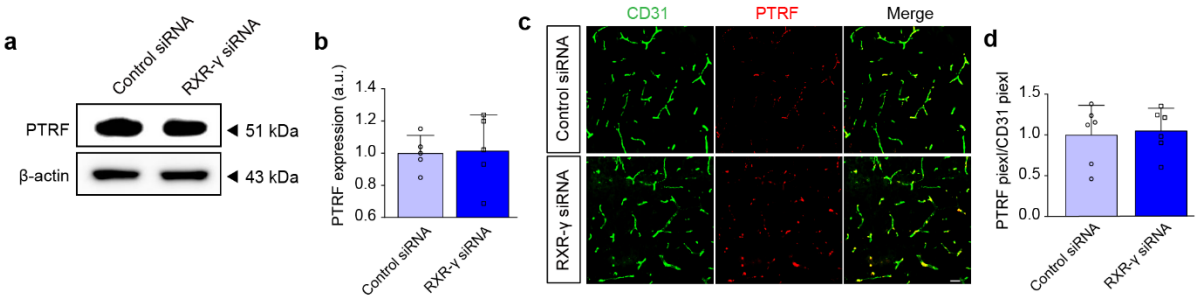

Supplemental Figure 11. Knockdown of RXR-γ does not change the level of caveolae.

(**a, b**) Quantitative analysis for immunoblotting of PTRF (a pool of 2 mice per sample; n = 5 samples per group; mean ± S.D; unpaired t-test). (**c**) Representative images of immunofluorescence staining of PTRF (red) in the cerebral microvessels ($CD31^+$, green) [quantified in (**d**); n = 6 in each group; mean ± S.D; unpaired t-test]. Scale bar: 20 μm.

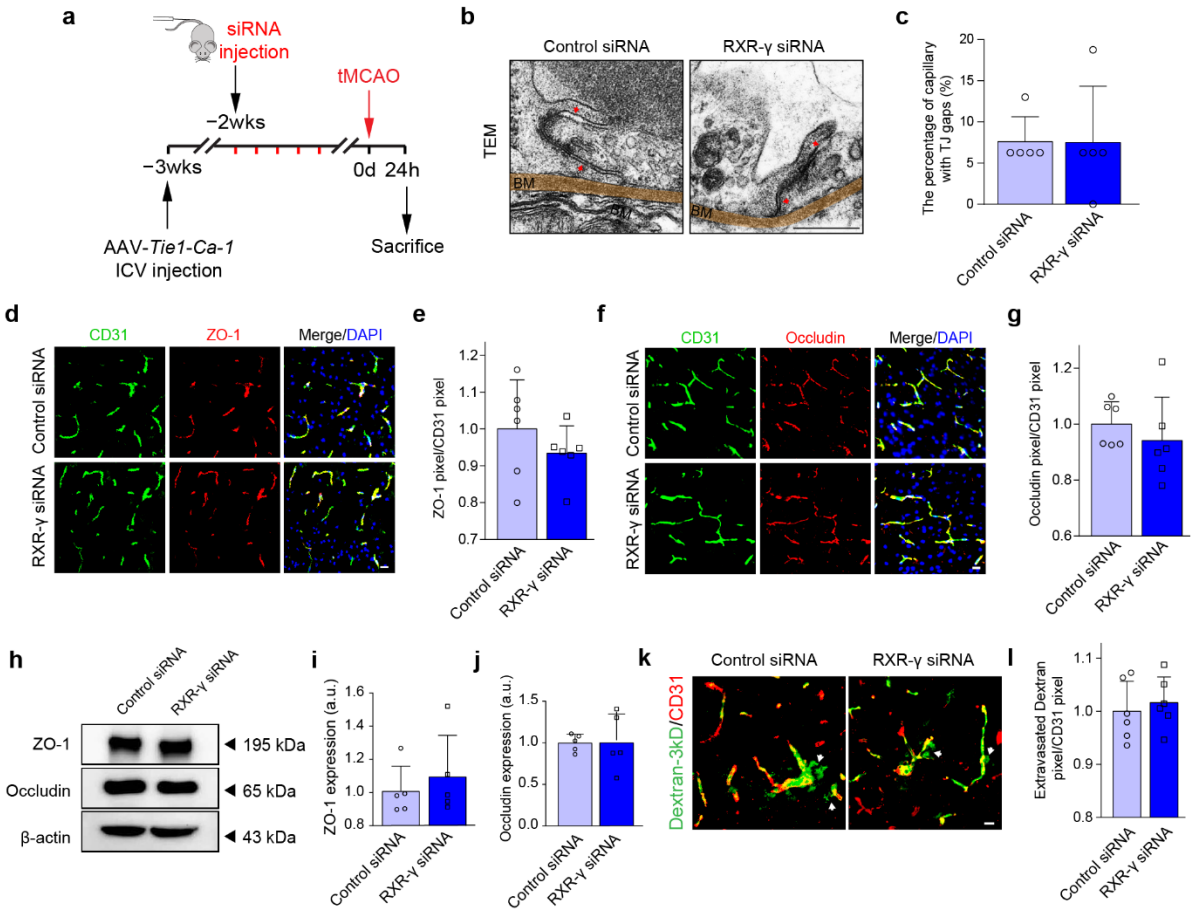

Supplemental Figure 12. Knockdown of RXR-γ did not affect TJ integrity and BBB leakage under Cav-1 overexpression.

(**a**) Experimental flow chart. (**b, c**) TEM images and quantification showing TJ gaps (red arrows) in the peri-infarct area 24h after tMCAO (n = 5 mice in each group. Sixteen capillaries were randomly chosen in each mouse; mean ± S.D; unpaired t-test). The red arrows indicate gaps between endothelial cells. (**d–g**) Immunofluorescence staining and quantifications showing the expression of ZO-1 (red) and occludin (red) in the CD31$^+$ vessels (green) (n = 6 in each group; mean ± S.D; unpaired t-test). (**h–j**) Immunoblotting and quantitative analysis of TJ proteins in microvascular segments (a pool of 2 mice per sample; n = 5 samples per group; unpaired t-test). (**K, L**) Representative images of immunofluorescence staining and quantification of extravasated FITC-dextran (3 kDa; white arrows) from CD31$^+$ microvessels (red) (n = 6 mice in each group; mean ± S.D; unpaired t-test). Scale bar: 500 nm in (**b**) and 20 μm in others. BM, basal membrane.

Table S1. Real-time PCR primers in this study.

Primer name	Primer sequence	
Cav-1	Forward	GAAGGGACACACAGTTTCG
	Reverse	AGGAAGGAGAGAATGGCAA
Spdef	Forward	GGCTCAACAAGGAGAAAGG
	Reverse	TGTAATACTGGCGGATGGA
Gpr65	Forward	TGGCAGATAAACCTCAAC
	Reverse	AGCATAGGACGAAAGTCA
Itih4	Forward	TATTACCTTGCCGCTTCC
	Reverse	CATACTTACCAGTCACCTCCA
Sis	Forward	CACTGAGCAGAATCCCTT
	Reverse	TGATGTGGCACTTCGTAT
Fgf21	Forward	CACCGCAGTCCAGAAAGT
	Reverse	TGGCTGTTGGCAAAGAAA
Slc17a9	Forward	TGCCCTGGAGACAACTAT
	Reverse	TGATGACTCTGTAACCCTGAC
Slc15a1	Forward	AGCGGCTACCAGTTCTTC
	Reverse	TGTTGGGTGGGATGTCTT
Lcn2	Forward	AAGGCAGCTTTACGATGT
	Reverse	TGGTTGTAGTCCGTGGTG
Rxrg	Forward	CGTGCTGTTTAACCCAGAT
	Reverse	AGGTGTTCCAGGCATTTC
Ido1	Forward	AGGATGCGTGACTTTGTG
	Reverse	TCTGGAAGATGCTGCTCT
Adra2b	Forward	CGTGCGTGGTGCGAGGTCTA
	Reverse	TTGATGCGGCGTGGAGTGC
GAPDH	Forward	AAGAAGGTGGTGAAGCAGG
	Reverse	GAAGGTGGAAGAGTGGGAGT

Table S2. Comparison of baseline data according to patients with and without ENI.

Variables	All patients, n = 270	With ENI, n = 100	Without ENI, n = 170	*P* value
Demographic characteristics				
Age, years	68.4 ± 12.4	66.7 ± 12.9	69.2 ± 12.2	0.099
Male, n (%)	171 (63.3)	68 (68.0)	103 (60.6)	0.222
Clinical data				
Hypertension	190 (70.4)	69 (69.0)	121 (71.2)	0.705
Diabetes mellitus	65 (24.1)	15 (15.0)	50 (29.4)	0.007
Hyperlipidemia	30 (11.1)	6 (6.0)	24 (4.1)	0.040
Systolic blood pressure, mmHg	137.2 ± 23.5	137.6 ± 24.9	136.5 ± 22.6	0.697
Diastolic blood pressure, mmHg	82.2 ± 14.7	81.6 ± 14.6	82.5 ± 14.7	0.622
Time from onset to recanalization, min	357.5 (251.0, 540.0)	351.0 (231.0, 532.5)	360.0 (270.0, 541.5)	0.312
Baseline NIHSS, score	13.0 (10.0, 16.0)	13.0 (11.0, 17.0)	12.0 (8.0, 16.5)	0.023
Baseline ASPECTS, score	9.0 (8.0, 9.0)	9.0 (8.0, 9.0)	8.0 (8.0, 9.0)	0.001
Prior intravenous thrombolysis, n (%)	119 (44.1)	48 (48.0)	71 (41.8)	0.319
Poor collateral status, n (%)	134 (49.6)	47 (47.0)	87 (51.2)	0.507
Caveolin-1 levels, ng/mL	0.191 (0.109, 0.298)	0.201 (0.136, 0.327)	0.178 (0.088, 0.278)	0.028

Abbreviations: ASPECTS, the Alberta Stroke Program Early Computed Tomography Score; NIHSS, National Institute of Health Stroke Scale.

Table S3. Physiological parameters and tMCAO-24h mortality in WT and *Cav-1*$^{-/-}$ mice.

Variables	WT mice	*Cav-1*$^{-/-}$ mice	*P* value
Weight, g	23.5 ± 0.9	23.8 ± 0.5	0.375
BP, mmHg	104.5 ± 5.6	106.2 ± 5.0	0.599
pH	7.38 ± 0.05	7.38 ± 0.03	0.846
Pco_2, mmHg	39.3 ± 2.2	39.8 ± 1.2	0.629
Po_2, mmHg	98.7 ± 2.7	99.2 ± 1.7	0.712
Bleeding time, s	55.2 ± 8.3	49.0 ± 10.5	0.285
tMCAO-24h mortality, %*	8.6	17.1	0.284

Values presented as Mean ± S.D. n = 6 mice in each group. * n = 35 in each group for calculating the mortality.